Hindawi Publishing Corporation
Journal of Nanomaterials
Volume 2016, Article ID 4086456, 9 pages
http://dx.doi.org/10.1155/2016/4086456

Research Article

Effect of an Albumin-Coated Mesoporous Silicon Nanoparticle Platform for Paclitaxel Delivery in Human Lung Cancer Cell Line A549

Yu Gao,[1,2,3] Xiaofang Che,[1,2] Chunlei Zheng,[1,2] Kezuo Hou,[1,2] Xiujuan Qu,[1,2] Yunpeng Liu,[1,2] and Zhitu Zhu[3]

[1]*Department of Medical Oncology, The First Hospital of China Medical University, Shenyang, Liaoning, China*
[2]*Key Laboratory of Anticancer Drugs and Biotherapy of Liaoning Province, The First Hospital of China Medical University, Shenyang, Liaoning, China*
[3]*Department of Oncology, The First Affiliated Hospital of Jinzhou Medical University, Jinzhou, Liaoning, China*

Correspondence should be addressed to Yunpeng Liu; cmuliuyunpeng@hotmail.com
and Zhitu Zhu; zhuzhitu@163.com

Received 14 July 2016; Revised 20 September 2016; Accepted 3 October 2016

Academic Editor: Martin J. Sweetman

Albumin-coated paclitaxel-mesoporous silicon nanoparticles (APMSN) were prepared to improve the anticancer effect in lung cancer by means of regulating the dissolution rate of paclitaxel (PTX). PTX was absorbed into the mesoporous structure of mesoporous silicon nanoparticles (MSN), which was defined as PMSN. PTX was proved to exist in an amorphous state in PMSN, which increased the dissolution rate of PTX. Albumin was coated on the surface of MSN to form AMSN; AMSN and PTX were mixed to form APMSN in order to achieve sustained release of PTX. Then, it was found that APMSN had more significant antiproliferate effects and induced more apoptotic proportion in comparison with PTX in A549 cells. Furthermore, the absorption mechanism of APMSN into A549 cells was investigated. Transmission electron microscopy (TEM) and laser scanning confocal microscopy (LSCM) showed that APMSN could cross the cell membrane and was taken into the cytoplasm quickly. Taken together, our results demonstrate that AMSN carriers have potential as nanodrug delivery systems in the treatment of lung cancer.

1. Introduction

In recent years, advances in nanotechnology have demonstrated that nanoparticles, generally ranging from 10 to 500 nm in size, can be used as effective drug transport delivery systems [1]. Nanoparticles can be made from different types of materials and include natural or synthetic polymer nanoparticles, liposomes, micelles, and silica nanoparticles [2]. Mesoporous silica nanoparticles (MSN) are very suitable carriers for nanodrug delivery systems due to their nanoscale size, relatively low density, good fluxility, and biocompatibility [3]. For nanoparticles made from mesoporous silica materials, it is well known that drug particle size can be decreased due to the spatial confinement of the mesoporous structure, and, as a result, the specific surface area of drug particles increases significantly. Therefore, the drug's solubility and dissolution rate can be enhanced according to the Ostwald–Freundlich and Noyes–Whitney equations. Moreover, the mesoporous structure could retain drug molecules in an amorphous form or in a microcrystalline state, thus inhibiting the aggregation of drug particles and further improving drug stability [4, 5].

It is well known that paclitaxel (PTX) is an effective drug for the treatment of solid tumors, such as lung cancer, ovarian cancer, breast cancer, and pancreatic cancer [6, 7]. However, PTX is insoluble in water, which seriously restricts the absorption of the drug [8, 9]. A nanodrug delivery system can transport anticancer drugs directly to the cancerous tissue

and effectively improve the absorption of water-insoluble drugs. A recent study has shown that porous silicon can improve the oral bioavailability of celecoxib *in vitro* and *in vivo* [10]. Wang et al. reported that modification of surface chemicals affected the release of an antibacterial drug from nanostructured porous silicon [11]. Furthermore, Wu et al. have demonstrated that novel synthesized dual-mesoporous silica nanospheres with core-shell structures can enhance the dissolution rate of poorly water-soluble drugs [12].

Although MSN can significantly improve the dissolution rate of a drug, it could also cause recrystallization of the dissolved drug to reduce the efficacy of the drug. Several ways are known to solve this problem. Chitosan-functionalized spherical nanosilica matrix is reported to be able to regulate the release rate of the poorly water-soluble drug carvedilol [13]. Additionally, osmotic pump technology could also be used to control the release rate of fenofibrate absorbed in mesoporous silica materials [14].

In this study, we used albumin-coated MSN (AMSN) as carriers in a nanodrug delivery system. Albumin is an endogenous human substance and therefore has good biocompatibility [15]. We predicted that when coated with albumin, an albumin-MSN-PTX delivery system (APMSN) would exhibit increased drug diffusion resistance and a decreased dissolution rate and obtained sustained release. So the APMSN increased drug absorption and improved the effect of PTX. Finally, through the solid state characterization of PTX in AMSN, MTT test, flow cytometry, and fluorescence microscopy, we sought to explore whether AMSN is suitable as a carrier for a nanodrug delivery system in the treatment of lung cancer.

2. Materials and Methods

2.1. Materials. PTX was provided by the Tianfeng Biotechnology Company (Xi'an, China, purity > 99%). Anhydrous ethanol, chromatographic acetonitrile, tetraethylorthosilicate (TEOS), styrene monomer, hexadecyltrimethylammonium bromide (CTAB), (3-aminopropyl)triethoxysilane (APTES), 2,2′-azobis[2-methylpropionamidine] dihydrochloride (AIBA), lysine, albumin, hypromellose, and octane were obtained from the Jin Zhou Xing Bei Reagent Company (Liaoning, China). 3-[4,5-Dimethylthiazol-2-yl]-2,5-diphenyltetrazolium bromide (MTT), annexin V-FITC, and propidium iodide (PI) were purchased from Nanjing KeyGEN Biotechnology Company (Jiangsu, China). 4,6-Diamidino-2-phenylindole (DAPI) was purchased from Shanghai Beyotime Company (Shanghai, China). Hoechst33342 and rhodamine-phalloidin were purchased from Shanghai Univ-Bio Company (Shanghai, China). Fluorescein isothiocyanate (FITC) and formaldehyde were purchased from Beijing Solarbio Company (Beijing, China). Deionized water was used in all experiments.

2.2. Cells and Cell Culture. Human lung adenocarcinoma A549 cells were obtained from the Type Culture Collection of the Chinese Academy of Sciences (Shanghai, China). Cells were cultured in RPMI 1640 medium (Sigma, USA) containing 10% fetal bovine serum (FBS), penicillin (100 U/mL), and streptomycin (100 mg/mL) at 37°C under an air atmosphere containing 5% CO_2.

2.3. Synthesis of MSN and MSN Coated by Albumin. MSN were prepared according to the process reported by Zhao et al. [16]. Briefly, the water phase (CTAB and water) and the oil phase (octane) were mixed to form an oil-in-water emulsion, and then monomeric styrene, lysine, TEOS, and AIBA were sequentially added to the emulsion at 60°C under an atmosphere of N_2. Styrene monomer (0.39–55 mg/mL) can regulate the pore size (5–16 nm). The reaction occurred at 60°C for 3 h and then remained at room temperature for 12 h. Particles were obtained by filtration and drying. The dried particles were calcined at 550°C to remove the templates. The MSN were obtained and stored in a dryer.

MSN surfaces were grafted with aminopropyl groups using APTES. Briefly, MSN (1 g) were placed into a three-necked flask and dehydrated at 100°C under a nitrogen atmosphere for 1 h. After that, APTES (4.0 mL) and ethanol (100 mL) were added to the system while stirring. Afterward, the samples were refluxed at 77°C under a nitrogen atmosphere for 12 h. The obtained product was washed three times with ethanol and dried at 90°C. The obtained MSN with amino groups (MSN-ap) were stored in a dryer.

The principle of albumin coating of mesoporous silicon nanoparticles is based on electrostatic adsorption. The process is shown in Figure 1. At pH 7.4, an albumin molecule has more than 200 negative charges, whereas the MSN with amino groups are positively charged. Due to electrostatic interactions, the pores of MSN can be sealed by albumin. The coating process was performed as follows: albumin was dissolved in phosphate buffer (PBS, pH 7.4), and MSN with amino groups (300 mg) were suspended in the albumin solution (0.1 mg/mL) for 5 h while stirring. Afterward, the suspension was centrifuged at a speed of 10000 rpm, and the products were washed three times with deionized water, followed by three washes with anhydrous alcohol. The residue containing albumin-encapsulated MSN was dried at 60°C under vacuum. The obtained samples (AMSN) were stored in a dryer.

2.4. Drug Loading Procedure. The anticancer drug PTX, used here as a model drug, was loaded into AMSN using the impregnation-adsorption method (Figure 1). AMSN and PTX (mass ratio of 1 : 1) were mixed and dispersed in dichloromethane. The system was stirred at room temperature for 24 h until the adsorption process reached equilibrium. Finally, the powder samples (APMSN) were obtained by centrifugation and dried in a vacuum for 24 h. PTX was extracted from an accurately weighed amount of APMSN with methanol. The drug content was determined by high-performance liquid chromatography (HPLC L-2400, HITACHI, Japan). All measurements were performed in triplicate. The drug loading procedure for MSN and MSN-ap was the same as that of APMSN. Drug-loaded samples of MSN and MSN-ap were defined as PMSN and PMSN-ap. PMSN and PMSN-ap were used for comparison with APMSN for *in vitro* dissolution experiments in order to show

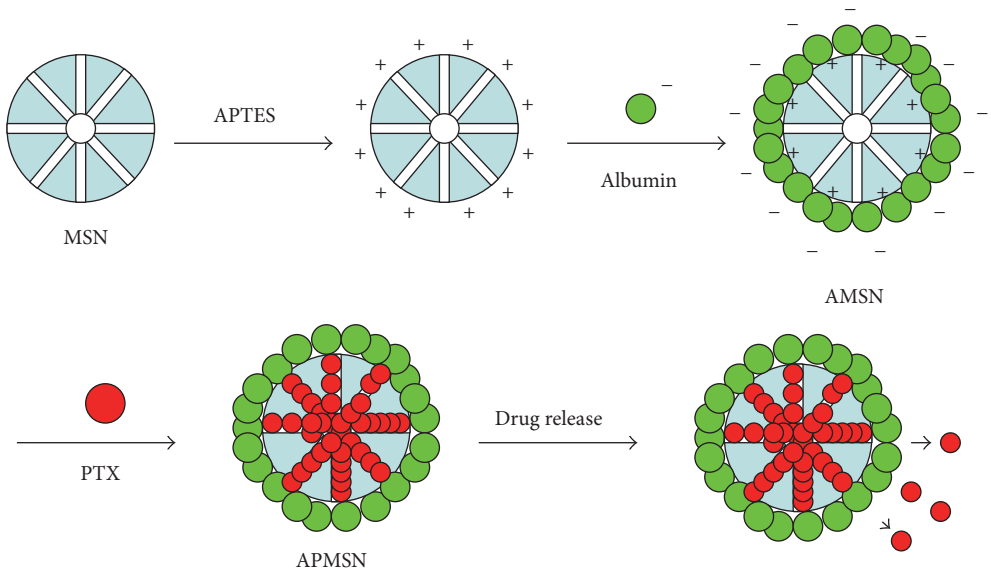

Figure 1: Preparation scheme of AMSN and APMSN.

the effect of MSN on improving the dissolution of PTX. The equation about the calculation of drug content is as follows: Drug Loading Capacity (DLC%) = PTX in APMSN weight/APMSN weight × 100%.

2.5. Characterization of MSN, AMSN and APMSN. The structure and morphology of carriers were characterized by scanning electron microscopy (SEM) (JEOL JSM-7001F, operated at 20 kV) and transmission electron microscopy (TEM) (Tecnai G2F30 operated at 200 kV). The thermal analysis of PTX was carried out by differential scanning calorimetry (DSC) (DSC-60, Shimadzu, Japan) from 30°C to 300°C at a heating rate of 10°C/min under a nitrogen atmosphere. X-ray diffraction analysis (XRD) (RigakuUltima IV, Japan) was used to evaluate the crystal changes of PTX in AMSN. The scanning rate was 4°/min over a range from 3° (2θ) to 60° with a step length of 0.02°.

2.6. In Vitro Drug Dissolution. A dissolution apparatus with magnetic stirring (DF-1, JintanYoulian Instrument Research Institute) was used for dissolution testing, and the dissolution medium was composed of phosphate buffer (pH 7.4). A certain amount of PMSN-ap and PMSN powder containing an equivalent of 0.7 mg raw PTX was, respectively, placed into 200 mL of dissolution medium at 37°C and stirred with a paddle speed of 100 rpm/min. Dissolution medium (2 mL) was withdrawn at 5, 10, 15, 20, 30, 45, and 60 min and passed through a 0.22 μm microporous membrane filter for HPLC analysis. APMSN powder containing an equivalent of 0.7 mg PTX was placed into 200 mL of dissolution medium at 37°C and stirred with a paddle speed of 100 rpm/min. Dissolution medium (2 mL) was withdrawn at 2, 4, 8, 12, 24, 36, 48, 72, 96, 120, 144, 168, 192, and 216 h and passed through a 0.22 μm microporous membrane filter. The drug content was analyzed by HPLC at a wavelength of 227 nm. The mobile phase consisted of acetonitrile and water (50 : 50, V/V).

2.7. In Vitro Cytotoxicity Assay. The MTT assay was used to assess mitochondrial activity of the cell by thiazolyl blue tetrazolium bromide. A549 cells (at a density of 3000 cells/well) were seeded in 96-well plates. Various concentrations of AMSN, PTX, and APMSN were dispersed in serum-free 1640 culture medium containing 2% hypromellose and added to 96-well plates. The suspension was withdrawn after an incubation period of 72 h. Then, 20 μL of MTT solution (5 mg/mL) was added to each well, and the cells were incubated for an additional 4 h at 37°C. Lastly, 200 μL of DMSO was added to each well, and the optical density (OD) was measured using a microplate reader (Tecan, Swiss) at 490 nm.

2.8. Flow Cytometry Analysis. Apoptosis was detected by flow cytometry (Becton Dickinson, CA). A549 cells (1×10^5 cells/well) were seeded in 6-well plates and incubated overnight. PTX and APMSN with concentrations of 5 ng/mL and 10 ng/mL, respectively, were added to the 6-well plates. After 48 h of incubation, A549 cells were harvested by trypsinization. Cells were collected by centrifugation and resuspended in 200 μL of binding buffer. Annexin V-FITC (5 μL) and PI (5 μL) were added, and the cells were incubated for 15 min in the dark. The apoptosis rate of A549 cells was evaluated by flow cytometry (Becton Dickinson, CA).

2.9. Morphological Observation of Apoptosis. A549 cells (1×10^5 cells/well) were seeded in 6-well plates. The next day, the RPMI 1640 medium was replaced, and various concentrations of PTX or APMSN were added to each well. After 48 h of incubation, A549 cells were fixed in a 4% formaldehyde PBS solution. After 30 min, the fixed cells were stained with DAPI. The presence of apoptotic cells was determined based on cell morphology as observed by fluorescence microscopy (Olympus, Japan).

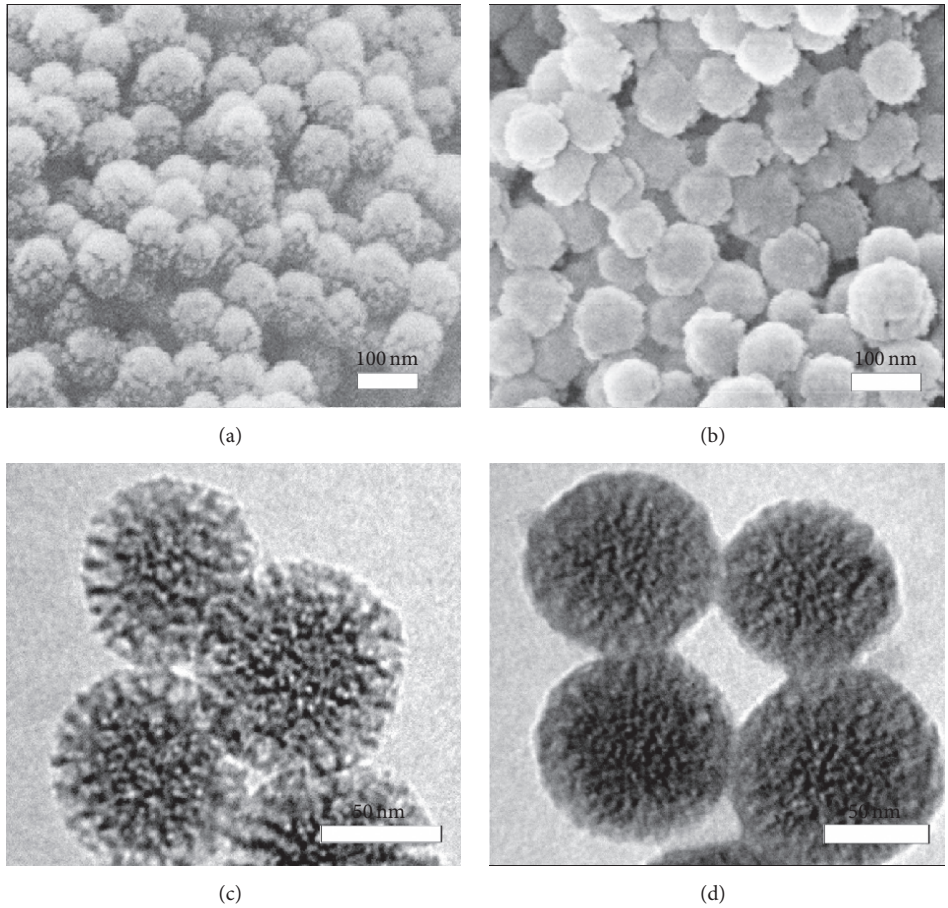

Figure 2: The SEM micrographs of the MSN (a) and AMSN (b); TEM micrographs of the MSN (c) and AMSN (d).

2.10. Laser Scanning Confocal Microscopy (LSCM) Observation of AMSN Uptake in Cells. FITC can combine with amino groups on the surface of AMSN. Fluorescently labeled AMSN was defined as FAMSN. FAMSN (50 μg/mL) were added to A549 cells (1×10^5 cells/well) for 0.5, 1, or 2 h. Then, A549 cells were washed three times with PBS and fixed in a 4% formaldehyde PBS solution. After removing the formaldehyde solution, the A549 cells were incubated in a PBS solution containing 0.1% Triton X-100 and 10% bovine serum albumin. The cell nuclei were stained with Hoechst33342 in a PBS solution for 10 min, and then the actin cytoskeletons were stained by rhodamine-phalloidin in a PBS solution for 20 min. Finally, evaluation of FAMSN uptake into cells was performed by laser scanning confocal microscopy (Olympus, Japan).

2.11. Transmission Electron Microscopy (TEM) Study of Nanoparticle Uptake. A549 cells (1×10^5 cells/well) were seeded in 6-well plates. The 1640 culture medium was removed after 24 h to allow for cell attachment. Drug-free AMSN (50 μg/mL) were dispersed in serum-free 1640 culture medium and added to 6-well plates. After 4 h of incubation, the suspension was removed, and the cells were washed three times with PBS. A549 cells were then collected, fixed with a 2% glutaraldehyde PBS solution for 24 h, and embedded in 2% agarose gel. Lastly, cells were fixed in a 4% osmium tetroxide solution and were embedded in epoxy resin after dehydration. After polymerization at 60°C for 24 h, the resin block was sliced using an ultramicrotome (Leica, Germany), and the obtained ultrathin sections were examined by TEM.

3. Results and Discussion

3.1. Structure Characteristics and Drug Loading. SEM images revealed the porous appearance of MSN and demonstrated that the MSN average particle size was 100 nm (Figure 2(a)). The TEM image in Figure 2(c) showed the mesoporous structure with a radial pattern. The pore size was approximately 7 nm, which is a suitable size for decreasing the particle size of poorly water-soluble drugs. The space limiting effects of nanometer-scale pores could restrict drug particles into nanometer-scale spaces and prevent agglomeration of drug particles [1]. Furthermore, high drug dispersity in a mesoporous structure could significantly improve the physical stability of the drug [17]. Images of AMSN were shown in Figures 2(b) and 2(d). It was obvious that a layer of albumin was present at the surface of the particles due to electrostatic adsorption. Albumin has a hydrodynamic diameter of

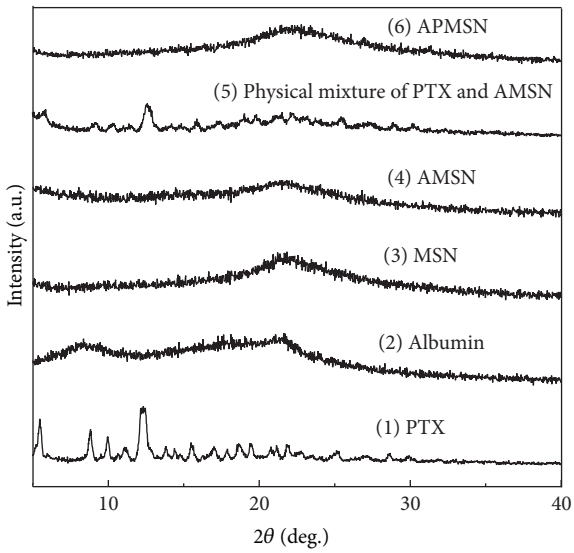

Figure 3: XRD profiles of PTX (1), albumin (2), MSN (3), AMSN (4), physical mixtures (5) of PTX and AMSN, and APMSN (6).

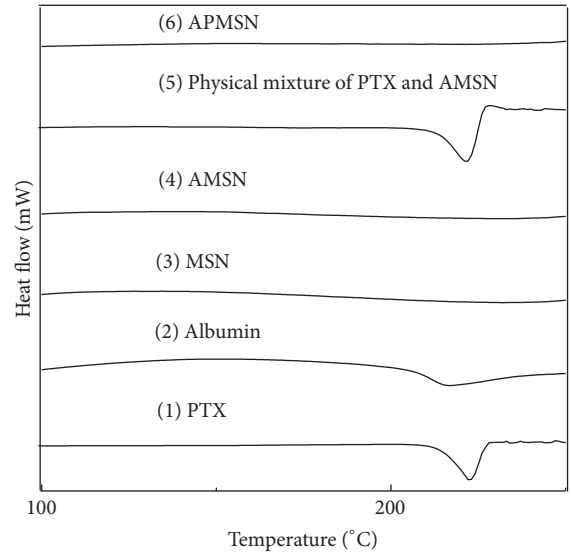

Figure 4: DSC profiles of PTX (1), slbumin (2), MSN (3), AMSN (4), physical mixtures (5) of PTX and AMSN, and APMSN (6).

14 nm × 4 nm × 4 nm [18], so albumin could only be adsorbed at the entrance of pores. The albumin-coated layer could increase the diffusion resistance of a drug and produce a sustained release effect.

The drug content of APMSN was 37.65 ± 0.149%. The loading capacity of AMSN depended on the PTX concentration and increased at higher PTX concentrations, but when the PTX concentration exceeded 300 mg/mL, the drug adsorption capacity of AMSN remained stable. Therefore, 300 mg/mL PTX was chosen as the optimal concentration to obtain maximum adsorption. These data suggested that AMSN had a good adsorption capacity as a carrier of poorly water-soluble drugs.

3.2. Solid State Characterization. X-ray diffraction analysis (XRD) results demonstrated that the PTX adsorbed into the mesoporous structure was in an amorphous form. As seen in Figure 3, the characteristic peak of raw PTX was at 12.6°. In contrast, no crystalline PTX was detected in APMSN, whereas a peak at 12.6° was observed in a physical mixture with the same proportion of PTX and AMSN. The absence of distinctive peaks in APMSN was attributed to the amorphous state of PTX loaded into AMSN. The DSC results also supported the conclusions of XRD. The endothermic peak of raw PTX was at 221°C (Figure 4). However, no PTX melting peak was displayed in the DSC curves of APMSN. In contrast, the endothermic peak of the physical mixture with the same proportion of PTX and AMSN was observed at 221°C. This confirmed that PTX absorbed in AMSN was in an amorphous state, which has direct implications for the solubility of PTX. The combined results of XRD and DSC further proved that the space restriction imposed by the mesoporous structure significantly inhibited the crystallinity of PTX, causing amorphous PTX to be highly dispersed in the mesoporous channels.

3.3. In Vitro Drug Dissolution. The effect of structural features on the dissolution of PTX was shown in Figure 5. The cumulative dissolution of PMSN at 10 min reached 80%, while APMSN reached 80% dissolution after 120 h. Obviously, the dissolution rate of PTX in MSN was significantly improved due to the nanometer-sized pores, large specific surface area, and the spatial confinement effect of the mesoporous structure. Furthermore, according to the dissolution behavior of PMSN-ap, amino chemical process of MSN had no effect on the dissolution of PTX. After albumin-coated MSN were prepared, the dissolution rate was effectively decreased. As a result, showed sustained release effect, which could prevent the recrystallization of drugs. Albumin is an endogenous substance, meaning MSN coated by albumin can make it prolonged time in circulation system.

3.4. In Vitro Cytotoxicity Assay. AMSN concentrations ranging from 12.5 μg/mL to 500 μg/mL were selected for toxicity evaluation. A549 cells were incubated with various concentrations of AMSN for 72 h. As seen in Figure 6(a), incubation with 500 μg/mL AMSN resulted in a slight reduction in cell viability and no more than 4% apoptosis in the A549 cell line. These data indicated that AMSN has good biocompatibility and no toxicity. According to the increased absorption and lower toxicity of AMSN, an AMSN system may be a suitable candidate for lung cancer treatment.

The MTT assay results for PTX- and APMSN-treated cells were shown in Figure 6(b). Treatment with APMSN (from 10 ng/mL to 320 ng/mL) for 72 h resulted in a significant reduction in cell viability compared to treatment with PTX (from 10 ng/mL to 320 ng/mL). The IC50 dose was 46.76 ± 0.46 ng/mL for APMSN at 72 h and 109.2 ± 4.84 ng/mL for PTX. These results demonstrated that APMSN had significant *in vitro* antiproliferative effects compared to treatment

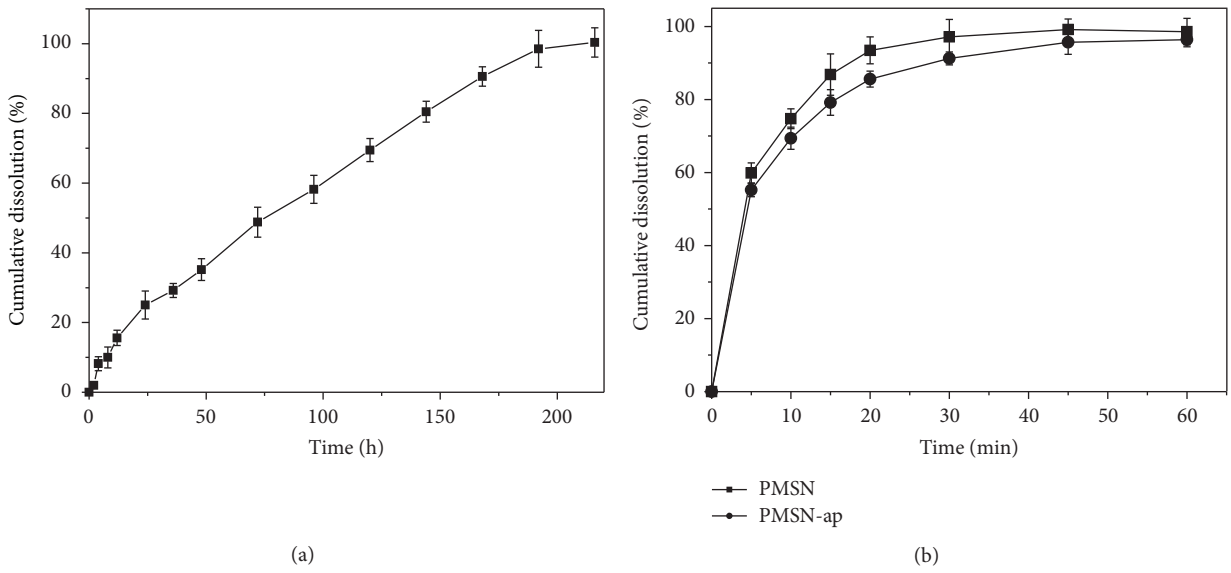

Figure 5: *In vitro* drug percentage cumulative dissolution profiles of APMSN (a), PMSN (b), and MSN-ap (b) ($n = 3$).

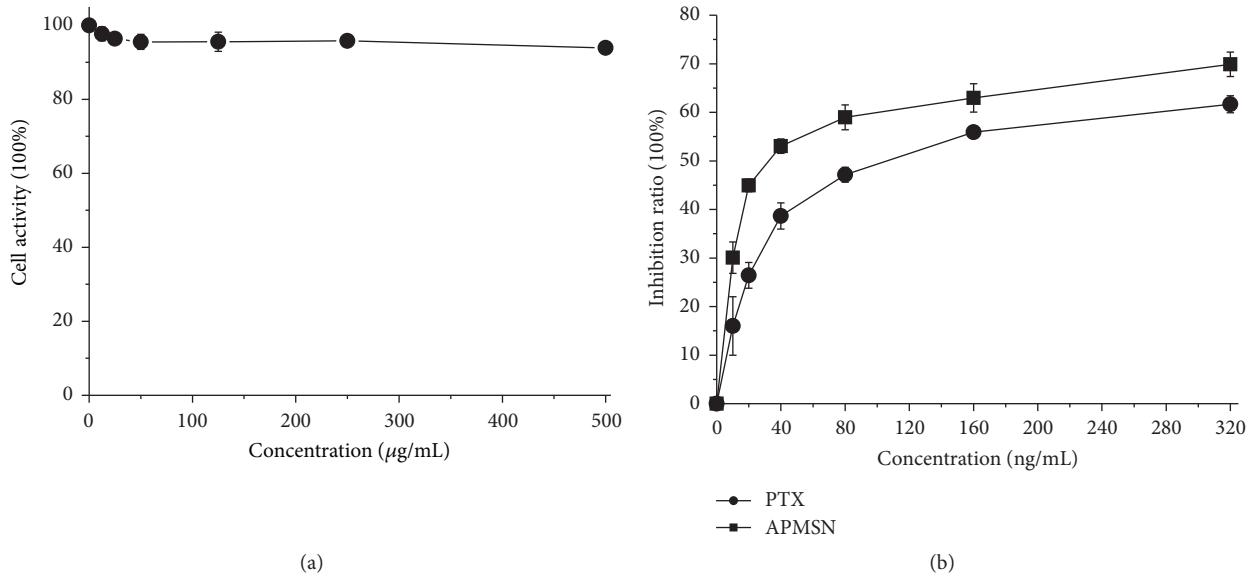

Figure 6: MTT results of AMSN (a) and PTX and APMSN (b) for evaluating carrier toxicity and cell inhibition rate of drug loading system ($n = 3$).

with PTX. Due to the nanoscale properties of AMSN, adsorption of PTX was increased significantly, which led to the enhancement of the antiproliferative effects of PTX. With an enhanced antitumor effect and lower toxicity, APMSN appears to be a suitable choice for lung cancer treatment.

3.5. Analysis of Apoptosis. As shown in Figure 7, the apoptosis rate of APMSN (5 ng/mL) was 34.39 ± 11.82% compared to 9.11 ± 2.33% for PTX (5 ng/mL). When the APMSN concentration was increased to 10 ng/mL, the apoptotic population was 45.95 ± 16.18%, and, correspondingly, the apoptosis rate at 10 ng/mL PTX was 22.90 ± 11.63%. Based on these data, it was obvious that APMSN can induce apoptosis in A549 cells and that the apoptosis rate was closely related to drug concentration. Furthermore, the apoptosis rate of APMSN-treated cells was higher than that of cells treated with PTX. The analysis of apoptosis based on cell morphology further confirmed the above results. Fluorescence microscopy images in Figure 7 show that the nuclei of cells treated with APMSN or PTX present shrinkage and fragmentation, while the nuclei of untreated cells display uniform, complete, blue fluorescence. With an increase in the PTX concentration from

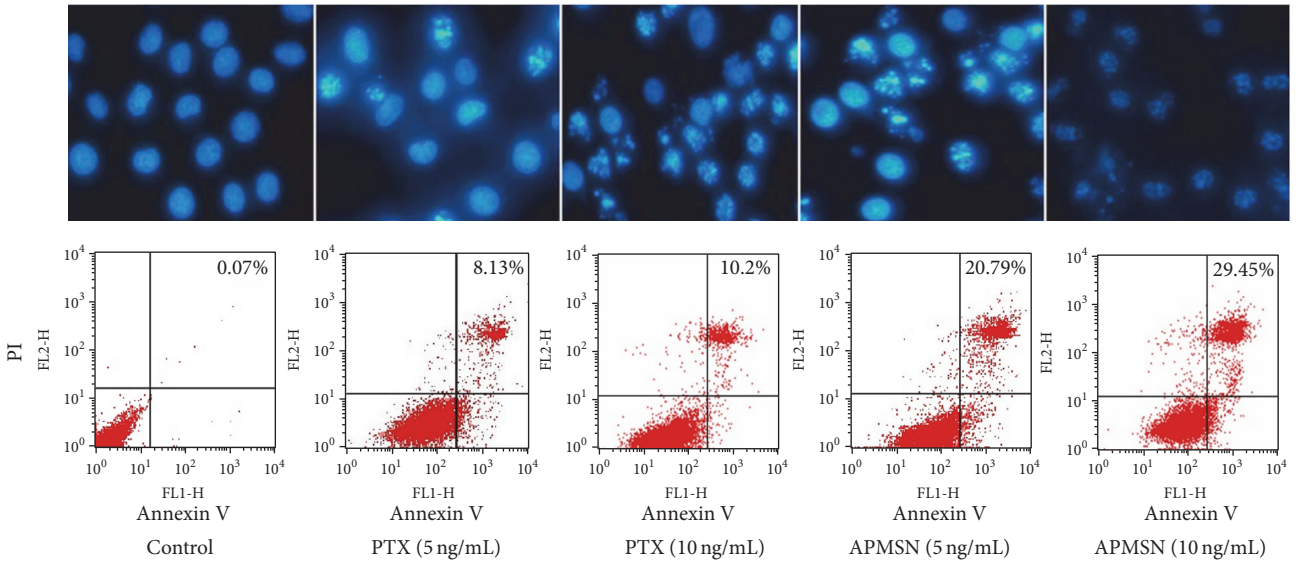

Figure 7: Apoptosis results and fluorescence microscope images of PTX and APMSN for evaluating effect of drug loading system on A549 cells ($n = 3$).

5 ng/mL to 10 ng/mL, the level of apoptosis increased notably. The number of apoptotic cells among APMSN-treated cells increased significantly relative to PTX-treated cells. The EPR effect (enhanced permeability and retention effect) is one of the characteristics of tumors. The rapid growth of the tumor tissue leads to tumor vascular abnormality and high vascular permeability; therefore, nanoparticles of 10–200 nm can penetrate the tumor tissue vessel wall and accumulate in tumor tissue [19]. Because of the EPR effect, the circulation of a nanoscale drug system may act to enhance the drug concentration in tumor tissue [20, 21].

3.6. The Uptake of FAMSN into A549 Cells. According to the LSCM results, the transport of FAMSN in A549 cells was time-dependent. As shown in Figures 8(a), 8(b), and 8(c), A549 cells were incubated with FAMSN (50 μg/mL) in serum-free RPMI 1640 medium for 0.5 h, 1 h, and 2 h at 37°C. LSCM observations showed that the uptake of FAMSN gradually increased with the extension of time. At 0.5 h, there were only a few FAMSN in A549 cells; when 1 h and 2 h had passed, more particles were observed in A549 cells. However, FAMSN did not transport into the nucleus but did aggregate in the cytoplasmic region. The intracellular distribution of FAMSN was further investigated by TEM. As shown in Figures 8(d) and 8(e), FAMSN was taken up into A549 cells by endocytosis. Untreated cells and FAMSN-treated cells were shown in Figures 8(d) and 8(e), respectively. With the extension of time, FAMSN accumulated in the cytosolic compartment or in vesicles. These results further suggested that the cellular uptake mechanism of FAMSN maybe include phagocytosis, nonspecific diffusion, and/or endocytosis. Moreover, with the added of advantages of nanoscale delivery, the drug loading and incubation times were proportional to the amount of drug in the cells, which is one of the reasons for APMSN-accelerated cell apoptosis.

4. Conclusions

We successfully prepared albumin-coated mesoporous silicon nanoparticles (AMSN) to improve the solubility of PTX. AMSN were suitable drug carriers due to their good biocompatibility, hydrophilicity, and lack of toxicity. Because of the space confinement inherent to the AMSN structure, PTX was present in an amorphous state in APMSN. The APMSN delivery system resulted in sustained drug release compared to a PMSN delivery system. Additionally, cell apoptosis in cells treated with APMSN was greater than that in cells treated with PTX because APMSN transferred more PTX into A549 cells due to the nanoscale properties of APMSN. Based on these studies, AMSN is a promising carrier to enhance the absorption of poorly water-soluble drugs.

Competing Interests

The authors declare that there is no conflict of interests regarding the publication of this paper.

Acknowledgments

This work was supported by the National Science and Technology Major project of the Ministry of Science and Technology of China (Grant no. 2013ZX09303002), Science and Technology Plan project of Liaoning Province (Grant no. 2014225013), National Natural Science Foundation of China (Grant no. 81372546), and Liaoning BaiQianWan Talents Program (Grant no. 2014921032).

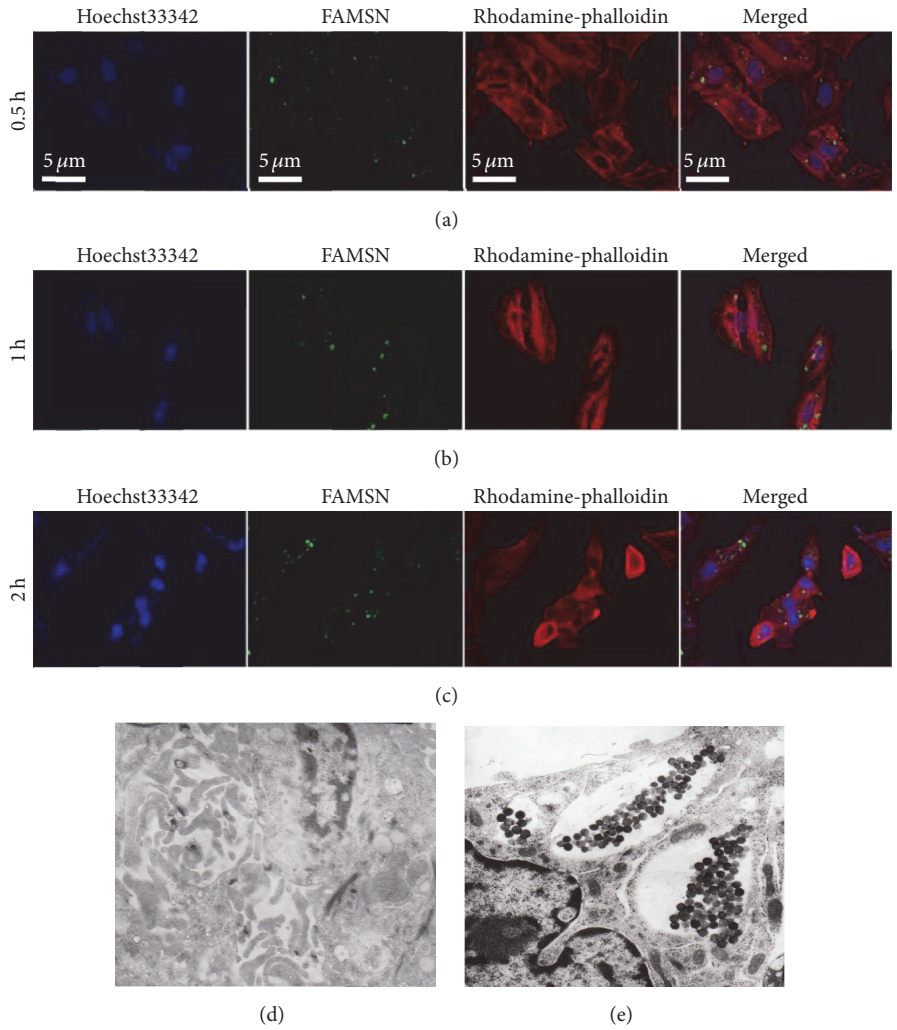

Figure 8: Cell uptake results of FAMSN in A549 cells (a, b, and c was the LSCM images at 0.5, 1, and 2 h after administrated 50 μg/mL of FAMSN and FITC was used as a fluorescent probe; d and e TEM images).

References

[1] F. Tang, L. Li, and D. Chen, "Mesoporous silica nanoparticles: synthesis, biocompatibility and drug delivery," *Advanced Materials*, vol. 24, no. 12, pp. 1504–1534, 2012.

[2] S. Baek, R. K. Singh, D. Khanal et al., "Smart multifunctional drug delivery towards anticancer therapy harmonized in mesoporous nanoparticles," *Nanoscale*, vol. 7, no. 34, pp. 14191–14216, 2015.

[3] Z. Zhao, Y. Gao, C. Wu, Y. Hao, Y. Zhao, and J. Xu, "Development of novel core-shell dual-mesoporous silica nanoparticles for the production of high bioavailable controlled-release fenofibrate tablets," *Drug Development and Industrial Pharmacy*, vol. 42, no. 2, pp. 199–208, 2016.

[4] M. J. K. Thomas, I. Slipper, A. Walunj et al., "Inclusion of poorly soluble drugs in highly ordered mesoporous silica nanoparticles," *International Journal of Pharmaceutics*, vol. 387, no. 1-2, pp. 272–277, 2010.

[5] M. Van Speybroeck, R. Mellaerts, R. Mols et al., "Enhanced absorption of the poorly soluble drug fenofibrate by tuning its release rate from ordered mesoporous silica," *European Journal of Pharmaceutical Sciences*, vol. 41, no. 5, pp. 623–630, 2010.

[6] S. S. Ramalingam, M. Shtivelband, R. A. Soo et al., "Randomized phase II study of carboplatin and paclitaxel with either linifanib or placebo for advanced nonsquamous non-small-cell lung cancer," *Journal of Clinical Oncology*, vol. 33, no. 5, pp. 433–442, 2015.

[7] J. A. Yared and K. H. R. Tkaczuk, "Update on taxane development: new analogs and new formulations," *Drug Design, Development and Therapy*, vol. 6, pp. 371–384, 2012.

[8] A. Cirstoiu-Hapca, F. Buchegger, N. Lange, L. Bossy, R. Gurny, and F. Delie, "Benefit of anti-HER2-coated paclitaxel-loaded immuno-nanoparticles in the treatment of disseminated ovarian cancer: therapeutic efficacy and biodistribution in mice," *Journal of Controlled Release*, vol. 144, no. 3, pp. 324–331, 2010.

[9] J.-H. Kim, Y. Kim, K. H. Bae, T. G. Park, J. H. Lee, and K. Park, "Tumor-targeted delivery of paclitaxel using low density lipoprotein-mimetic solid lipid nanoparticles," *Molecular Pharmaceutics*, vol. 12, no. 4, pp. 1230–1241, 2015.

[10] J. Riikonen, A. Correia, M. Kovalainen et al., "Systematic in vitro and in vivo study on porous silicon to improve the oral

bioavailability of celecoxib," *Biomaterials*, vol. 52, no. 1, pp. 44–55, 2015.

[11] M. Wang, P. S. Hartman, A. Loni, L. T. Canham, N. Bodiford, and J. L. Coffer, "Influence of surface chemistry on the release of an antibacterial drug from nanostructured porous silicon," *Langmuir*, vol. 31, no. 22, pp. 6179–6185, 2015.

[12] C. Wu, X. Sun, Z. Zhao et al., "Synthesis of novel core-shell structured dual-mesoporous silica nanospheres and their application for enhancing the dissolution rate of poorly water-soluble drugs," *Materials Science and Engineering C*, vol. 44, pp. 262–267, 2014.

[13] L. Sun, Y. Wang, T. Jiang et al., "Novel chitosan-functionalized spherical nanosilica matrix as an oral sustained drug delivery system for poorly water-soluble drug carvedilol," *ACS Applied Materials & Interfaces*, vol. 5, no. 1, pp. 103–113, 2013.

[14] C. Wu, Z. Zhao, Y. Zhao, Y. Hao, Y. Liu, and C. Liu, "Preparation of a push-pull osmotic pump of felodipine solubilized by mesoporous silica nanoparticles with a core-shell structure," *International Journal of Pharmaceutics*, vol. 475, no. 1, pp. e298–e305, 2014.

[15] M. Jupin, P. J. Michiels, F. C. Girard, M. Spraul, and S. S. Wijmenga, "NMR identification of endogenous metabolites interacting with fatted and non-fatted human serum albumin in blood plasma: fatty acids influence the HSA-metabolite interaction," *Journal of Magnetic Resonance*, vol. 228, pp. 81–94, 2013.

[16] Z. Zhao, C. Wu, Y. Zhao, Y. Hao, Y. Liu, and W. Zhao, "Development of an oral push-pull osmotic pump of fenofibrate-loaded mesoporous silica nanoparticles," *International Journal of Nanomedicine*, vol. 10, pp. 1691–1701, 2015.

[17] Y. Chen, W. Yang, B. Chang, H. Hu, X. Fang, and X. Sha, "In vivo distribution and antitumor activity of doxorubicin-loaded N-isopropylacrylamide-co-methacrylic acid coated mesoporous silica nanoparticles and safety evaluation," *European Journal of Pharmaceutics and Biopharmaceutics*, vol. 85, no. 3, pp. 406–412, 2013.

[18] T. Wang, H. Jiang, Q. Zhao, S. Wang, M. Zou, and G. Cheng, "Enhanced mucosal and systemic immune responses obtained by porous silica nanoparticles used as an oral vaccine adjuvant: effect of silica architecture on immunological properties," *International Journal of Pharmaceutics*, vol. 436, no. 1-2, pp. 351–358, 2012.

[19] N. Bertrand, J. Wu, X. Xu, N. Kamaly, and O. C. Farokhzad, "Cancer nanotechnology: the impact of passive and active targeting in the era of modern cancer biology," *Advanced Drug Delivery Reviews*, vol. 66, pp. 2–25, 2014.

[20] H. Maeda, "Toward a full understanding of the EPR effect in primary and metastatic tumors as well as issues related to its heterogeneity," *Advanced Drug Delivery Reviews*, vol. 91, pp. 3–6, 2015.

[21] T. Stylianopoulos and R. K. Jain, "Design considerations for nanotherapeutics in oncology," *Nanomedicine: Nanotechnology, Biology, and Medicine*, vol. 11, no. 8, pp. 1893–1907, 2015.